Optimization of an Inverse Convection Solution Strategy

Joseph R VanderVeer, Yogesh Jaluria*

Department of Mechanical and Aerospace Engineering: Rutgers University, 98 Brett Rd, Piscataway NJ, 08854

Abstract

Keywords: Inverse Problems, Computational Heat Transfer, Convection

1. Introduction

Thermal-fluid systems often create situations where the engineering problem is an inverse heat transfer problem. These problems often have limited physical access, very limited to no boundary condition knowledge, and/or limited domain knowledge.

For example, the temperature distribution of an optical fiber drawing furnace is difficult to measure directly due to shape, inaccessibility, and high temperatures. The center of the furnace is easily accessible and this directly leads to an inverse heat transfer problem. Issa et al. [1] [1] developed a regularization technique utilizing the centerline temperature from which the wall temperature may be obtained.

Another example, is the inverse plume in a crossflow problem. The problem entails solving for the plume boundary conditions utilizing limited domain knowledge. A novel predictor-corrector method was developed by VanderVeer and Jaluria [2] [2] to solve such a problem.

The present work is the logical progression of the inverse plume in a crossflow problem, the inverse jet in a crossflow problem. The inverse jet in a crossflow problem has many more practical applications and ...

*Corresponding Author
Email address: jaluria@soemail.rutgers.edu (Yogesh Jaluria)

Nomenclature

$\boldsymbol{r}$	vector location of sampled points
a	number of sample locations used in the predictor stage
b, m	model parameters
$C_1, C_2, C_{1\epsilon}, C_\mu, \sigma_k, \sigma_\epsilon$	$k-\epsilon$ model coefficients
d	number of simulations
E	thermal energy
F	minimization function
k, ϵ	turbulence kinetic energy, dissipation rate
l, I	turbulence length scale and intensity
n	number of sample locations
P	pressure
P_{rt}	turbulent Prandtl number
T	temperature
t	time
U	free stream velocity
X, Y	normalized coordinates
x, y	coordinates

Greek Symbols

$\boldsymbol{\Delta}$	relative difference between the first sampled point and other sampled points
$\boldsymbol{\delta}$	vector distance between the actual sampled location and the current test location
λ	thermal conductivity
μ	dynamic viscosity
μ_t	eddy viscosity
ϕ	normalized temperature $\phi = \frac{T-T_\infty}{T_S-T_\infty}$
ρ	density
ε	error associated with the inverse convection method at a location with given sampled data

Superscripts

$*$	predictor stage, alternative heat flux eqn.

Subscripts

$0, 1, 2$	sample point indexes
∞	free stream
A, B	data set A,B
i, j, k	index
mod	modified
O	optimized
P	predicted
S	source

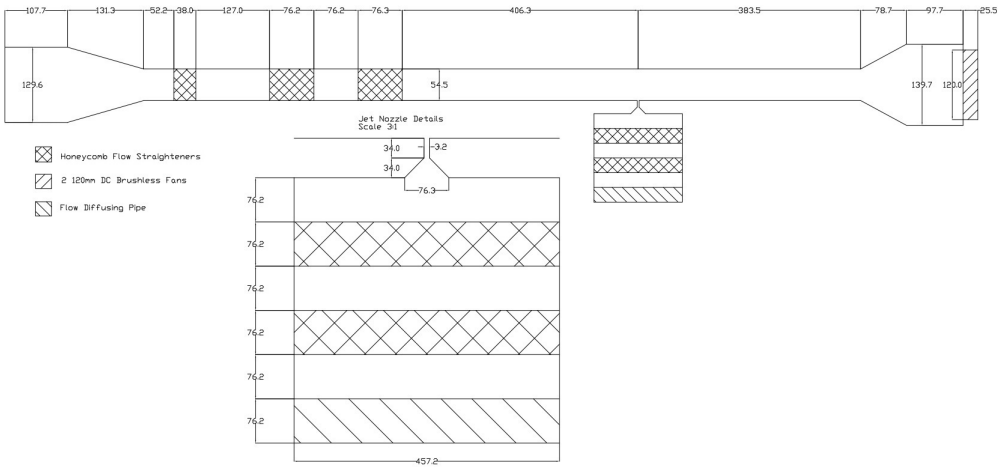

Figure 1: Schematics of the wind tunnel and jet

2. Experimental System

The experiment consists of a wind tunnel with a surface level jet located within the test section. The jet uses compressed air passed through flow straighteners to achieve a velocity of U_S and is heated to temperature T_S. The jet is subjected to a perpendicular crossflow of velocity U_∞. Figure 1 is a diagram of the wind tunnel and jet, dimensions are in millimeters.

The wind tunnel test section dimensions are $54.5 \times 305 \times 254\,mm$. The maximum velocity of the wind tunnel is $5.0\,m/s$. The jet is heated by electric cartridge heaters (Omega AHP-7561) with a maximum temperature of $425\,K$ due to material limitations of the wind tunnel. The X-direction is directed downstream of the wind tunnel with the zero at the center of the jet. The Y-direction is in the direction of the jet and is zero at the surface of the wind tunnel. Due to the large aspect ratio of the wind tunnel the flow is assumed to be two-dimensional.

The free stream velocity is determined by a Pitot-Static tube attached to a NIST traceable differential pressure sensor from Omega(PX655-0.1DI). The pressure sensor has a full scale reading of 0.1 inches of water and is accurate to 0.05% of full scale. This results in a maximum of 3% error of the calculated velocity.

The jet velocity is determined utilizing a rotameter and verified using a

Pitot-Static tube attached to the same previously described pressure sensor. This results in the same amount of error of 3% for the jet velocity.

The temperature of domain is measured using a K-type thermocouple mounted to an X-Y traversing stage. Sampled data over the course of several days indicate repeatability of the experiment to within 2%.

3. Numerical Simulations

The simulations were all performed using Ansys Fluent[3]. The Navier-Stokes equations were solved using a three-dimensional, steady state, realizable $k-\epsilon$ model with enhanced wall effects. Conjugate heat transfer is modelled. The free stream Reynolds number is of order 6×10^3, while the jet Reynolds number is between 10^3 and 10^4. The Rayleigh number is of order 10^7.

The governing equations are expressed below:

$$u_i = \overline{u_i} + u_i^{'} \tag{1}$$

$$\frac{\partial \rho}{\partial t} + \frac{\partial}{\partial x_i}\left(\rho u_i\right) = 0 \tag{2}$$

$$\begin{aligned} &\frac{\partial}{\partial t}\left(\rho u_i\right) + \frac{\partial}{\partial x_j}\left(\rho u_i u_j\right) = \\ &\qquad \frac{\partial P}{\partial x_i} + \frac{\partial}{\partial x_j}\left[\mu\left(2S_{ij} - \frac{2}{3}\delta_{ij}\frac{\partial u_k}{\partial x_k}\right) - \rho\overline{u_i^{'}u_j^{'}}\right] \end{aligned} \tag{3}$$

$$\begin{aligned} &\frac{\partial}{\partial t}\left(\rho E\right) + \frac{\partial}{\partial x_i}\left[u_i\left(\rho E + P\right)\right] = \\ &\qquad \frac{\partial}{\partial x_i}\left[\left(\lambda + \frac{C_p \mu_t}{P_{rt}}\right)\frac{\partial T}{\partial x_i}\right] \end{aligned} \tag{4}$$

$$\begin{aligned} &\frac{\partial}{\partial t}\left(\rho k\right) + \frac{\partial}{\partial x_j}\left(\rho k u_j\right) = \\ &\qquad \frac{\partial}{\partial x_j}\left[\left(\mu + \frac{\mu_t}{\sigma_k}\right)\frac{\partial k}{\partial x_j}\right] + \frac{\partial u_j}{\partial x_i}\left(-\rho\overline{u_i^{'}u_j^{'}}\right) \\ &\qquad - g_i \frac{\mu_t}{\rho P_{rt}}\frac{\partial \rho}{\partial x_i} + \rho\epsilon \end{aligned} \tag{5}$$

$$\frac{\partial}{\partial t}(\rho\epsilon) + \frac{\partial}{\partial x_j}(\rho\epsilon u_j) = \frac{\partial}{\partial x_j}\left[\left(\mu + \frac{\mu_t}{\sigma_\epsilon}\right)\frac{\partial \epsilon}{\partial x_j}\right] + \rho C_1 S\epsilon - \rho C_2 \frac{\epsilon^2}{k + \sqrt{\nu\epsilon}} - C_{1\epsilon}\frac{\epsilon}{k} C_{3\epsilon} g_i \frac{\mu_t}{\rho P_{rt}}\frac{\partial \rho}{\partial x_i} \tag{6}$$

$$-\rho\overline{u_i' u_j'} = 2\mu_t S_{ij} - \frac{2}{3}\delta_{ij}\left(\rho k + \mu_t \frac{\partial u_k}{\partial x_k}\right) \tag{7}$$

The constants for the turbulence model are [4, 5] :

$$C_{1\epsilon} = 1.44, C_2 = 1.9, \sigma_k = 1.0, \sigma_\epsilon = 1.2, P_{rt} = 0.85 \tag{8}$$

$$C_1 = max\left[0.43, \frac{Sk/\epsilon}{Sk/\epsilon + 5}\right], S = \sqrt{2S_{ij}S_{ji}}, C_{3\epsilon} = tanh\left(\frac{u_g}{u_p}\right) \tag{9}$$

$$\mu_t = \frac{\rho C_\mu k^2}{\epsilon} \tag{10a}$$

$$C_\mu = \frac{1}{A_0 + \frac{A_1 k U^*}{\epsilon}} \tag{10b}$$

$$U^* \equiv \sqrt{S_{ij}S_{ji} + \Omega_{ij}\Omega_{ji}} \tag{10c}$$

$$A_0 = 4.04 \tag{10d}$$

$$A_1 = \sqrt{6} cos\left[\frac{1}{3} cos^{-1}\left(\sqrt{6}\frac{S_{ij}S_{jk}S_{ki}}{(S_{ij}S_{ji})^{\frac{3}{2}}}\right)\right] \tag{10e}$$

$$S_{ij} = \frac{1}{2}\left(\frac{\partial u_i}{\partial x_j} + \frac{\partial u_j}{\partial x_i}\right) \tag{10f}$$

$$\Omega_{ij} = \frac{1}{2}\left(\frac{\partial u_i}{\partial x_j} - \frac{\partial u_j}{\partial x_i}\right) \tag{10g}$$

Where the u_g and u_p are the velocity component parallel and perpendicular to gravity respectively.

The inflow boundary conditions are:

$$u = U_\infty, v = 0, T = T_\infty, P = P_\infty, l = 4mm, I = 5\% \tag{11a}$$

$$k = \frac{3}{2}\left(U_\infty I\right)^2 \tag{11b}$$

$$\epsilon = C_\mu^{3/4}\frac{k^{3/2}}{l} \tag{11c}$$

4. Inverse Solution Methodology

5. Results and discussions

6. Conclusions

References

[1] J. Issa, Z. Yin, C. E. Polymeropoulos, Y. Jaluria, Temperature distribution in an optical fiber draw tower furnace, Journal of Materials Processing and Manufacturing Science vol 4 (1996) 221–232.

[2] J. VanderVeer, Y. Jaluria, Solution of an inverse convection problem by a predictor-corrector approach, International Journal of Heat and Mass Transfer vol65 (2013) 123–130.

[3] Ansys, Fluent (version 13), 2010.

[4] T. hsing Shih, W. Liou, A. Shabbir, Z. Yang, J. Zhu, A new $k-\epsilon$ eddy viscosity model for high reynolds number turbulent flows, Computer Fluids vol 24 (1995) 227–238.

[5] Ansys, Fluent Technical Documents v14.0, Technical Report, Ansys, 2011.